

phys. stat. sol. (a) **145**, 539 (1994)

Subject classification: 68.55; S1.61; S5.11

*Fakultät für Physik der Universität Bielefeld<sup>1)</sup> (a) and  
Max-Planck-Institut für Mikrostrukturphysik, Halle<sup>2)</sup> (b)*

## **Interface Stability and Silicide Formation in High Temperature Stable $\text{Mo}_x\text{Si}_{1-x}/\text{Si}$ Multilayer Soft X-Ray Mirrors Studied by Means of X-Ray Diffraction and HRTEM**

By

U. KLEINEBERG (a), H.-J. STOCK (a), A. KLOIDT (a), B. SCHMIEDESKAMP (a),  
U. HEINZMANN (a), S. HOPFE (b), and R. SCHOLZ (b)

Multilayer thin films consisting of alternating *pure* molybdenum and silicon layers with layer thicknesses of a few nanometers are of increasing interest for soft X-ray optical applications in the wavelength region above the Si-L edge ( $\lambda = 12.4$  nm). In order to enhance the thermal and long term stability, which is of great importance for applications with high power soft X-ray sources, interdiffusion of molybdenum and silicon as a mechanism of thermal destruction of the multilayer system has to be reduced. For this purpose multilayers with absorber layers of two different  $\text{Mo}_x\text{Si}_{1-x}$  mixtures,  $\text{Mo}_{0.5}\text{Si}_{0.5}/\text{Si}$  and  $\text{Mo}_{0.33}\text{Si}_{0.67}/\text{Si}$ , and a double-layer thickness of about 7 nm are prepared by electron beam evaporation in a UHV system. The thermal stability for both systems is studied by post deposition annealing at different temperatures. For each temperature interdiffusion and interfacial roughness of the multilayers are examined by small angle X-ray diffraction (SAXD) at  $\lambda = 0.154$  nm, while the formation of nanocrystallinities with lattice plane orientation parallel to the layer system is investigated by large angle X-ray diffraction (LAXD). In the case of the  $\text{Mo}_{0.5}\text{Si}_{0.5}/\text{Si}$  multilayer system these studies are completed by high resolution transmission electron microscopy (HRTEM) at multilayer cross sections and optical diffraction measurements (ODM).

### **1. Introduction**

Multilayers consisting of alternating molybdenum and silicon are used as soft X-ray mirrors above the Si-L edge ( $\lambda \geq 12.4$  nm) [1 to 5], where they exhibit normal-incidence reflectivities exceeding 60%. A main disadvantage of these systems is their poor thermal stability because they show a degradation of the Mo–Si multilayer structure at annealing temperatures between 400 and 600 °C [6 to 10]. The destruction mechanism is commonly attributed to interdiffusion of molybdenum and silicon at the interfaces followed by the nucleation and growth of silicides, which leads to a consumption of the silicon layers. In order to achieve thermal stability exceeding 600 °C, the interdiffusion has to be reduced and the influence of the silicide formation to the multilayer stability has to be investigated.

Multilayer soft X-ray mirrors consisting of alternating pure silicon layers (acting as low absorbing spacer layers) and molybdenum–silicon alloy layers of variable mixture (acting as absorber layers) exhibit a higher thermal stability up to 900 °C (probably because of the lower silicon concentration gradient in the double layer) and moderate normal incidence soft X-ray reflectivities, for example 46% at  $\lambda = 14$  nm for a  $\text{Mo}_{0.5}\text{Si}_{0.5}/\text{Si}$  multilayer (33 double layers) as deposited [11 to 13].

<sup>1)</sup> Postfach 1001 31, D-33501 Bielefeld, Federal Republic of Germany.

<sup>2)</sup> Weinberg 2, D-06120 Halle (Saale), Federal Republic of Germany.

This work mainly reports on the microstructure of these systems and their changes after annealing processes between 500 and 950 °C. The studies are performed using small and large angle X-ray diffraction and high resolution transmission electron microscopy (HRTEM).

## 2. Experimental Procedures

Three different types of multilayers with a double-layer thickness of about 7 nm are fabricated by electron beam evaporation in a UHV system (base pressure  $1 \times 10^{-8}$  Pa) on Si(100) or Si(111) substrates (100 mm diameter,  $T_{\text{sub}} = 175$  °C). Conventional Mo/Si multilayers are made by alternating evaporation of molybdenum and silicon from two different evaporation sources, while the  $\text{Mo}_x\text{Si}_{1-x}$  multilayers are fabricated by a continuous evaporation of silicon and an alternating evaporation of molybdenum. So the absorber layers in the  $\text{Mo}_x\text{Si}_{1-x}$  multilayers are prepared by simultaneous evaporation of molybdenum and silicon and the mixture of the absorber layers is adjusted by the rate regulation of the two different evaporation sources for Mo and Si, while the spacer layers consist of pure silicon. The evaporation rates of the different materials are measured by quartz oscillators and the individual layer thicknesses are controlled by in situ soft X-ray reflectivity measurements ( $\lambda = 4.47$  nm,  $\alpha = 70^\circ$ ).

After the deposition the multilayers have been annealed in a separate vacuum chamber ( $p = 5 \times 10^{-3}$  Pa). In order to avoid thermal accumulation effects, different pieces of the same multilayer have been annealed for 20 min at temperatures between 400 and 950 °C. The temperatures have been measured at the substrate holder with a NiCr/CuNi thermocouple.

All samples have been characterized by X-ray diffraction at  $\lambda = 0.154$  nm ( $\text{CuK}_\alpha$ ) using a conventional X-ray diffractometer setup. The multilayer structure is investigated by SAXD at grazing incidence angle  $\theta = 0$  to  $3^\circ$ . The nanocrystallinity of the layers has been measured by LAXD at grazing incidence angles  $\theta = 10$  to  $36^\circ$ . The multilayer structure as well as the individual layer structure have been investigated by HRTEM pictures of prepared multilayer cross sections using a JEOL 4000 EX electron microscope (400 kV) with a point resolution of 0.19 nm. Additional information about the crystallinity of the multilayer films has been concluded from optical diffraction measurements (ODM) taken from sample areas of about 90 nm diameter on HRTEM negatives. By using the diffraction spots from the Si substrate as a calibration, small crystalline phases containing only a few lattice planes can be identified by measuring their lattice spacings [14].

## 3. Experimental Results of the Mo/Si Multilayer

In this section we give a short summary of the results we have obtained for the structure of electron beam deposited Mo/Si multilayers. The multilayer structure of a Mo/Si multilayer consisting of  $N = 12$  double layers has been characterized by a small angle X-ray reflectivity measurement displayed in Fig. 1.

The measurement (solid line) has been simulated by a calculation (dashed line) based on the optical thin film theory using the Fresnel equations. Bulk values of the optical constants evaluated from the tabulated atomic scattering factors from Henke et al. [15] are used. The calculation has been carried out using the following multilayer model structure of twelve periods with a period thickness of 7.4 nm:

Each period consists of a four-layer structure with a 3.7 nm thick pure silicon layer, a 2.1 nm thick  $\text{Mo}_5\text{Si}_3$ -like interdiffusion layer (interlayer) at the Mo-on-Si interface, a 1 nm

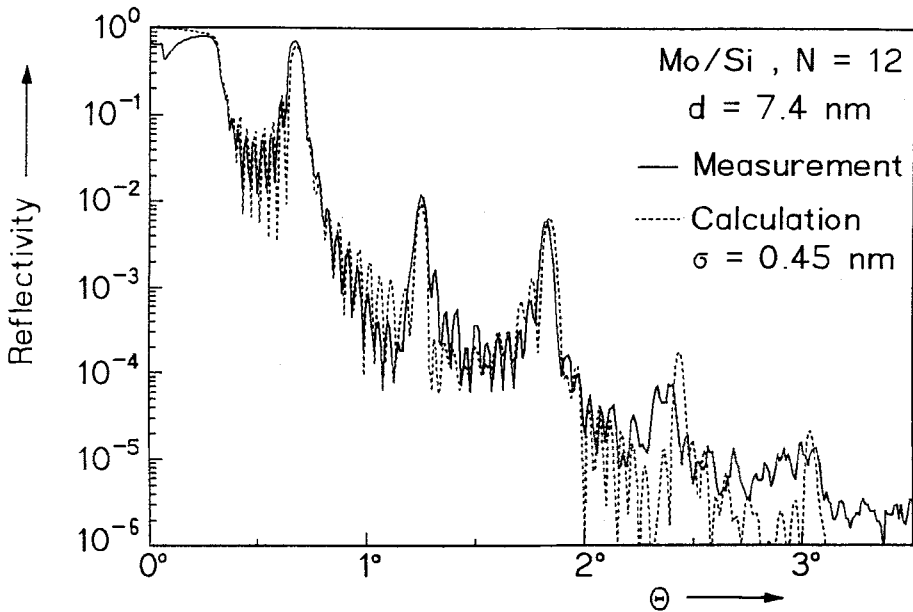


Fig. 1. Measured (solid) and calculated (dashed) small angle X-ray reflectivity of a Mo/Si multilayer deposited by UHV electron beam evaporation

thick pure molybdenum layer, and a 0.6 nm thick  $\text{Mo}_5\text{Si}_3$ -like interlayer at the Si-on-Mo interface. A Debye-Waller factor with a roughness parameter of  $\sigma = 0.45$  nm has been multiplied to the reflected amplitude from each boundary to fit the reduction of the measured X-ray reflectivity. Note that intensity ratios of the Bragg maxima in the measured SAXD data cannot be fitted by a calculation neglecting the formation of an interlayer at the Mo-Si interface. Further investigations of similar Mo/Si multilayers show that the thickness of this interdiffusion layer depends on the substrate temperature during the deposition process. The molybdenum-rich stoichiometry of the Mo-Si interlayer, which has been used in the simulation of the small angle X-ray reflectivity, has been measured by concentration depth profiling with Rutherford backscattering (RBS) [16, 17].

The occurrence of interfacial layers which relative sharp interfaces in the Mo/Si multilayer system is also displayed by cross sectional HRTEM pictures (Fig. 2) The picture shows the smooth natural silicon dioxide layer at the surface of the Si(100) substrate, followed by alternating (dark) molybdenum and (light) silicon layers (terminated by a silicon layer). All periods (with the exception of the first molybdenum layer onto the silicon dioxide layer, which acts as a diffusion barrier) show the existence of thick interfacial layers at the Mo-Si interfaces, while almost no interfacial layers exist at the Si-Mo interface. The reason for the asymmetry is given by molecular dynamic simulations, which show that the lighter Si atoms do not penetrate into the polycrystalline molybdenum layers, while the heavier Mo atoms penetrate into the porous structure of the amorphous silicon layers [18].

The thermal stability of the Mo/Si multilayer structure has been investigated by small angle X-ray reflectivity measurements at Mo/Si multilayer samples annealed for 20 min at different temperatures between 300 and 600 °C.

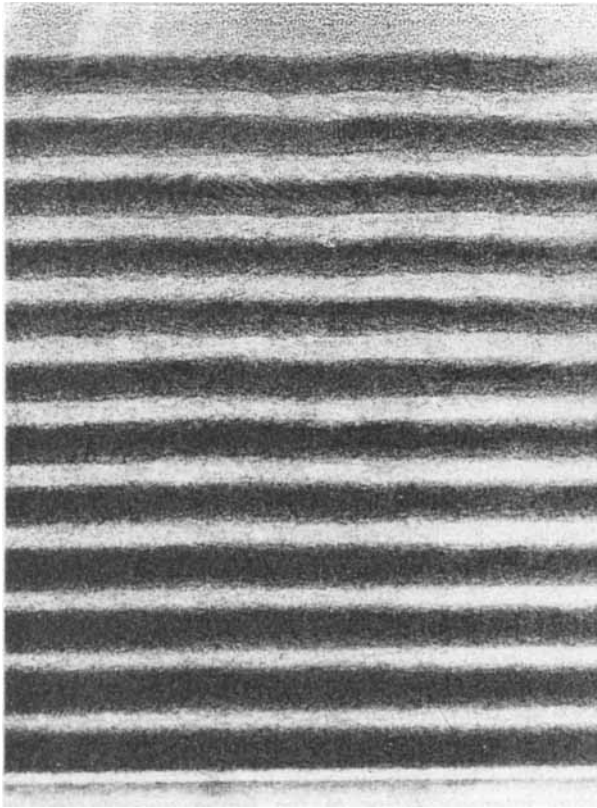


Fig. 2. High resolution cross sectional TEM picture of a Mo/Si multilayer

The measurements displayed in Fig. 3 show an almost undisturbed multilayer structure up to 500 °C, only a very small reduction of the double-layer thickness possibly due to structural relaxation [19 to 21] can be observed, which results in a very small angular shift of the Bragg maxima towards larger grazing angles  $\theta$ .

Between 500 and 550 °C the double-layer thickness of the Mo/Si multilayer is strongly reduced by about 20% due to interdiffusion in the multilayer stack and the reflectivities of the Bragg maxima are modified by a changing absorber-to-spacer thickness ratio. At 600 °C the intensities of the Bragg maxima are strongly reduced indicating the proceeding destruction of the Mo/Si multilayer.

The mechanism of the multilayer destruction between 500 and 600 °C has been examined by investigating the nanocrystallinity of the Mo/Si multilayer films performing large angle X-ray diffraction measurements (Fig. 4).

The measurement of the sample as deposited shows two sharp diffraction peaks resulting from the single-crystalline Si(111) substrate, additionally a broad Mo(110) diffraction peak at  $\theta = 20.2^\circ$  occurs due to diffraction from small Mo crystallites (b.c.c. structure), which show a preferential orientation with their Mo(110) lattice planes parallel to the layer system. This texture, which has also been found by other authors [22 to 25] results in an orientation of the closed-packed lattice planes of the b.c.c. crystallites parallel to the multilayer stack.

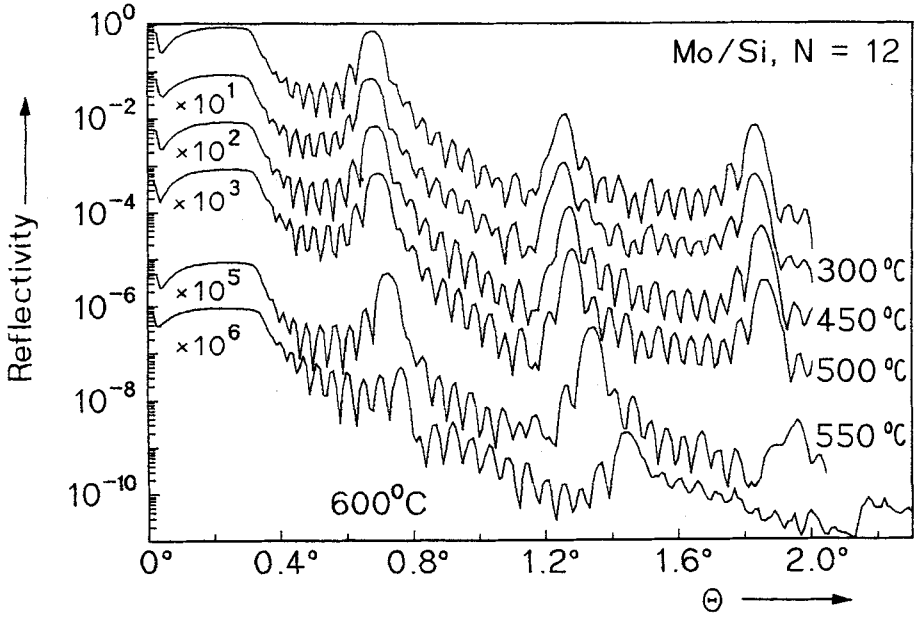


Fig. 3. Measured small angle X-ray reflectivity of a Mo/Si multilayer as deposited and after annealing at different temperatures between 300 and 600 °C

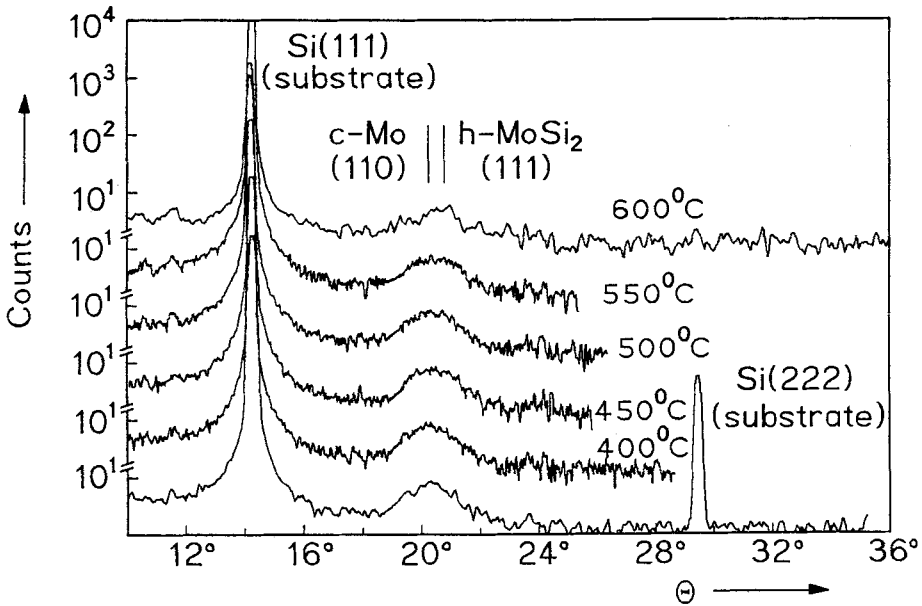


Fig. 4. Measured large angle X-ray diffraction of a Mo/Si multilayer after annealing at different temperatures between 400 and 600 °C

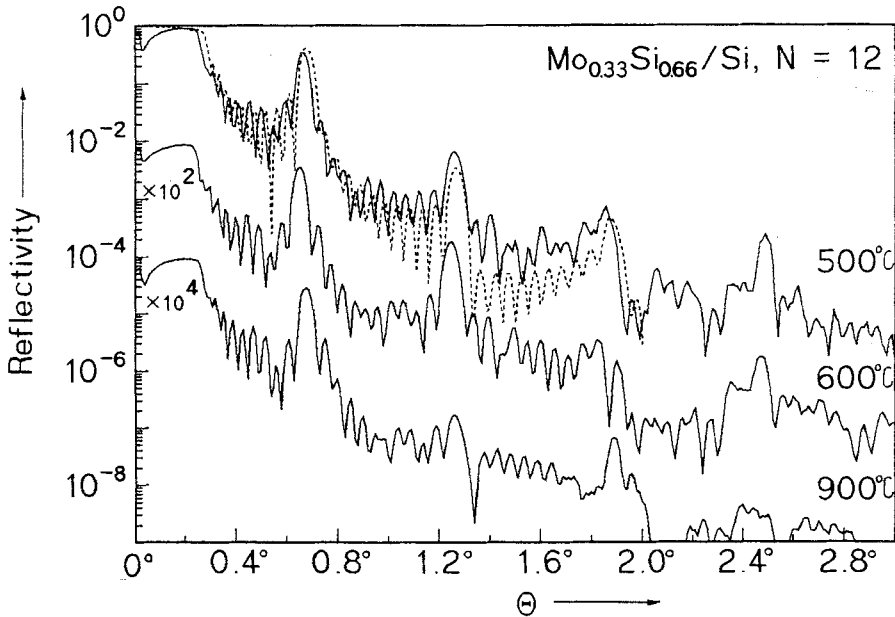


Fig. 5. Measured small angle X-ray reflectivity of a  $\text{Mo}_{0.33}\text{Si}_{0.66}/\text{Si}$  multilayer after annealing at different temperatures between 500 and 900 °C

The crystallite length perpendicular to the multilayer stack can be estimated from the peak width to about 2 nm, so the crystallites are almost limited to the pure molybdenum layers. As can be seen in the HRTEM picture the dimensions of the Mo crystallites parallel to the layer system strongly exceed their length perpendicular to the multilayer system.

The crystallinity of the multilayer does not change up to 500 °C, while at 600 °C a new peak at  $\theta = 20.5^\circ$  near to the vanishing Mo(110) maximum occurs, which can be identified (by JCPDS data files [26]) as diffraction from hexagonal  $\text{MoSi}_2$  (111) crystallites. Therefore, interdiffusion of the multilayer system between 500 and 550 °C, which leads to a consumption of the Si layers, is enhanced by the reaction and formation of h- $\text{MoSi}_2$  crystallites and results in a destruction of the multilayer system at 600 °C, where the crystallisation process has been observed [27].

#### 4. Experimental Results of the $\text{Mo}_{0.33}\text{Si}_{0.66}$ Multilayer

The structural properties of the multilayer system  $\text{Mo}_{0.33}\text{Si}_{0.66}/\text{Si}$  consisting of  $N = 12$  double layers as deposited and after annealing have been investigated by small angle X-ray diffraction and are displayed in Fig. 5. The simulation (dashed line) of the measured data of the sample as deposited (upper solid line) is based on a multilayer model structure consisting of  $\text{MoSi}_2$ -like absorber layers and Si spacer layers, in contrast to the Mo/Si multilayer system no interdiffusion layers are necessary to fit the measured data correctly. The layer thicknesses have been calculated directly from a simulation of the in situ C-K reflectivity measurements during the deposition process and result in a period thickness of  $d = 7.4$  nm. The interfacial roughness (Debye-Waller parameter) of the multilayer has been determined by a comparison with the calculation to  $\sigma = 0.6$  nm, which is slightly higher than in the case of the Mo/Si multilayer ( $\sigma = 0.45$  nm).

The multilayer remains undisturbed for annealing temperatures up to  $500^\circ\text{C}$  showing an unchanged small angle X-ray diffraction measurement as for the sample as deposited. A first variation of the multilayer structure occurs between  $500$  and  $600^\circ\text{C}$ . The angular positions of the Bragg peaks remain constant, indicating a constant period thickness, but their intensity relations vary. This can be explained by a slight variation of the thickness ratio  $\Gamma = d_{\text{absorber}}/d$  of the individual films. No further variation of the multilayer structure occurs between  $600$  and  $850^\circ\text{C}$ .

The complete destruction of the multilayer starts at  $900^\circ\text{C}$ , where an angular shift and a reduction of the main diffraction maxima indicate an interdiffusion of the multilayer stack leading to a smaller period thickness. Note that at  $950^\circ\text{C}$  no Bragg diffraction maxima can be observed any longer, indicating an almost completely destroyed multilayer stack.

The structural transformation of the multilayer system between  $T = 500$  and  $600^\circ\text{C}$  is again explained by a crystallisation process in the individual  $\text{Mo}_{0.33}\text{Si}_{0.66}$  absorber layers, which has been investigated by large angle X-ray diffraction (see Fig. 6). The X-ray diffraction intensity of the unannealed sample shows no indication of crystallites in the spacer and absorber layers, which is in contrast to similar measurements of Mo/Si multilayers, where strongly textured Mo(110) crystallites are found. The Si(200) and Si(400) peaks are contributions from the Si(100) substrate. No significant crystallisation process indicated by additional diffraction peaks can be observed up to  $500^\circ\text{C}$ . At  $600^\circ\text{C}$  a broad peak at  $\theta = 20.5^\circ$  occurs, which is identified as diffraction from small h-MoSi<sub>2</sub> (111) crystallites. The mean crystallite length of about 3 to 4 nm (perpendicular to the multilayer stack), estimated from the peak width, indicates that the crystallisation process is limited to the (mixed) absorber layers.

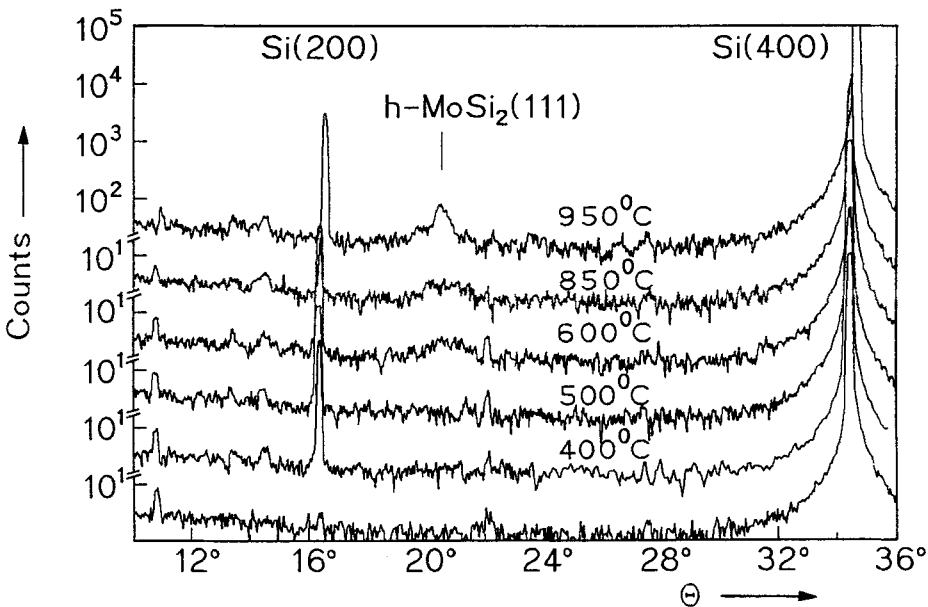


Fig. 6. Measured large angle X-ray reflectivity of a  $\text{Mo}_{0.33}\text{Si}_{0.66}/\text{Si}$  multilayer as deposited and after annealing at different temperatures between  $500$  and  $950^\circ\text{C}$

At higher temperatures up to 850 °C neither a growth of the h-MoSi<sub>2</sub> crystallites nor a recrystallisation of tetragonal MoSi<sub>2</sub> has been observed. At  $T = 950$  °C an increased crystallite length can be deduced from the smaller peak width, which is explained by a growth of h-MoSi<sub>2</sub> in the destroyed multilayer stack.

### 5. Experimental Results of the Mo<sub>0.5</sub>Si<sub>0.5</sub> Multilayer

The thermal stability of a Mo<sub>0.5</sub>Si<sub>0.5</sub>/Si multilayer alloy system with  $N = 33$  double layers evaluated from small angle X-ray diffraction data is displayed in Fig. 7.

In contrast to the Mo<sub>0.33</sub>Si<sub>0.66</sub>/Si multilayer, the double-layer thickness decreases between  $T = 500$  and 600 °C by about 10%, while simultaneously a growth of h-MoSi<sub>2</sub> crystallites in the absorber layers occurs.

The LAXD measurements of the annealed Mo<sub>0.5</sub>Si<sub>0.5</sub>/Si multilayer are very similar to those of the Mo<sub>0.33</sub>Si<sub>0.66</sub>/Si multilayer system in Fig. 6. Again the amorphous layer structure of the as deposited sample changes between 500 and 600 °C due to the crystallisation of h-MoSi<sub>2</sub>.

The decreasing period can be explained by an interdiffusion enhanced by the silicide formation, which strongly reduces the spacer layer thicknesses. This partial consumption of the spacer layers, which become thinner than the absorber layers, results in a thickness ratio  $\Gamma > 0.5$ . This is supported by the increasing second order reflectivity, while the first order reflectivity is reduced. After the crystallisation has occurred, the multilayer remains almost stable up to 850 °C and is destroyed at 900 °C.

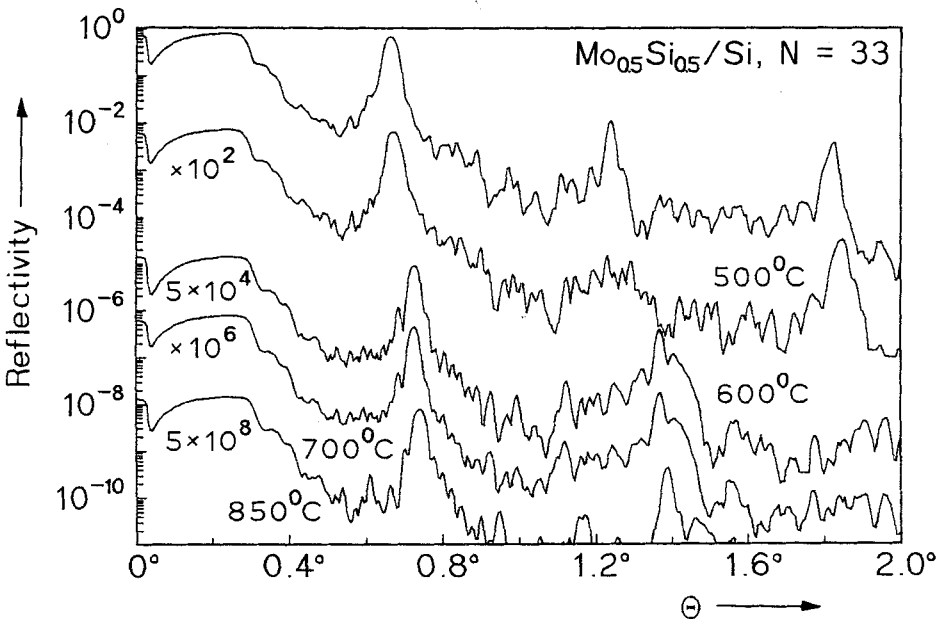


Fig. 7. Measured small angle X-ray reflectivity of a Mo<sub>0.5</sub>Si<sub>0.5</sub>/Si multilayer as deposited and after annealing at different temperatures between 500 and 850 °C

Additional information about the layer structure and the crystallinity of the films is given by cross sectional HRTEM investigations (Fig. 8) and the corresponding optical diffractograms of the HRTEM negatives (Fig. 9). The  $\text{Mo}_{0.5}\text{Si}_{0.5}/\text{Si}$  sample as deposited (Fig. 8a) shows a periodic layer structure consisting of amorphous layers with very smooth interfaces and almost no interfacial layers. The optical diffraction measurement (Fig. 9a) shows besides the sharp diffraction spots from the Si(100) substrate a diffuse diffraction ring typical for an amorphous layer structure.

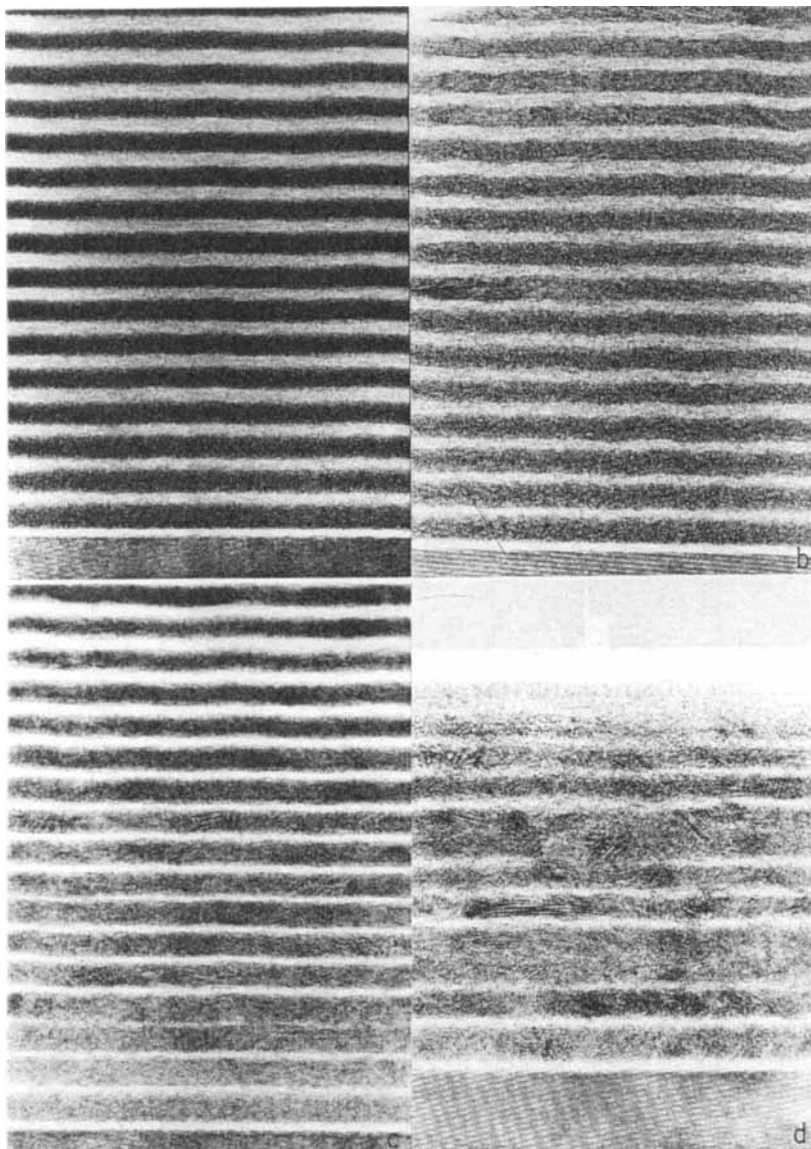


Fig. 8. High resolution cross sectional TEM pictures of a  $\text{Mo}_{0.5}\text{Si}_{0.5}/\text{Si}$  multilayer: a) as deposited, b) annealed at 500 °C, c) annealed at 700 °C, d) annealed at 850 °C

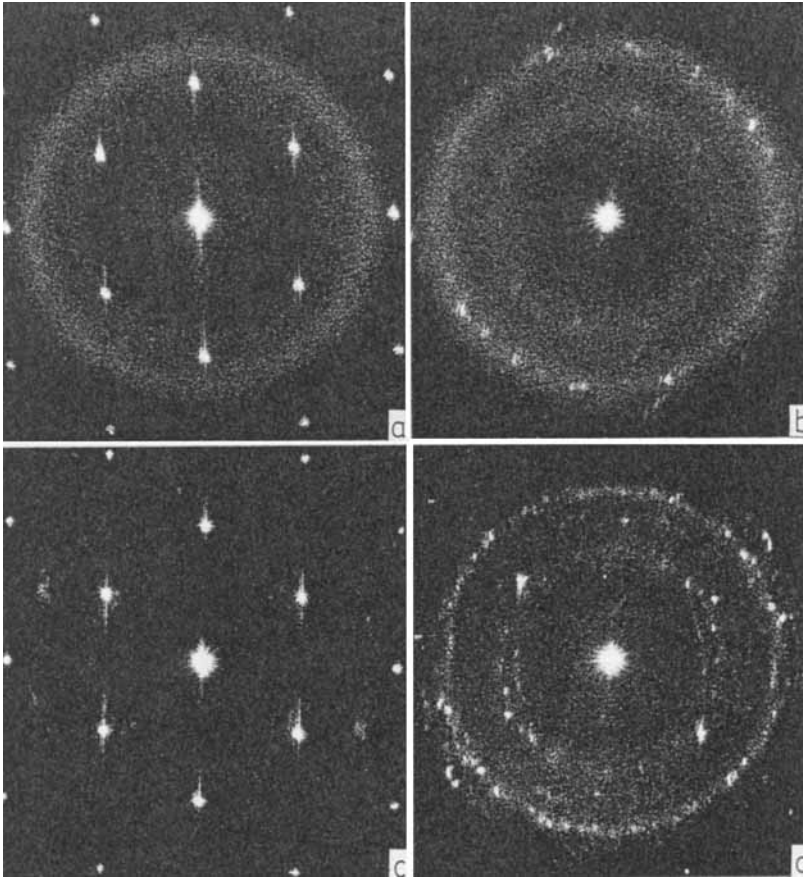


Fig. 9. Optical diffractograms (ODM) of the HRTEM negatives: a) as deposited, b) annealed at 500 °C, c) annealed at 700 °C, d) annealed at 850 °C

The interdiffusion process at lower temperatures is illustrated in the HRTEM picture (Fig. 8b) by the thinner silicon spacer layers in the case of the sample at  $T_{\text{bak}} = 500$  °C, compared to the sample as deposited. The nucleation of small crystallites at this temperature, which cannot be detected by X-ray diffraction, is also illustrated. The occurrence of sharper diffraction rings and some diffraction spots in the ODM picture (Fig. 9b) clearly displays the starting  $\text{MoSi}_2$  crystallisation process. These crystallites are primarily detected in the upper parts of the multilayer system, so that no contributions from substrate diffraction occur in this ODM picture. This discrepancy between X-ray diffraction data and HRTEM picture might be caused by a crystallisation process induced by the thinning of the sample cross sections by ion-milling as well as by some very few  $\text{MoSi}_2$  crystallites in the annealed sample, which might be present at this temperature and cannot be detected by X-ray diffraction.

The picture of the sample at  $T = 700$  °C (Fig. 8c) displays the rapid decrease of the spacer layers as well as the (lateral) growth of the h- $\text{MoSi}_2$  crystallites. Some silicon layers near the substrate are almost totally consumed by the interdiffusion process, but most of the

multilayer system remains stable after the silicide reaction up to 850 °C (Fig. 8d). The ODM picture of the sample annealed at 850 °C (Fig. 9d) displays the proceeding crystallisation in the whole multilayer stack by more intense and sharp rings and spots. The positions of the three most intense ring structures agree with various lattice spacings of the hexagonal  $\text{MoSi}_2$  crystal structure.

## 6. Conclusions

$\text{Mo}_x\text{Si}_{1-x}/\text{Si}$  multilayer soft X-ray mirrors show high thermal stability up to 900 °C, while  $\text{Mo}/\text{Si}$  multilayers of the same period thickness are destroyed at 600 °C. Interdiffusion of Mo and Si occurs until all Mo is consumed into  $\text{MoSi}_2$ . The interfacial roughness of the  $\text{Mo}_x\text{Si}_{1-x}$  multilayer system is not substantially modified by the crystallisation of the h- $\text{MoSi}_2$ , which occurs for all systems between 500 and 600 °C.

## Acknowledgements

We would like to thank Dr. Mai (IWS, FhG Dresden) and co-workers for their fruitful cooperation. This work is financially supported by BMFT (13N5539 and 13N5994) and Fa. Carl Zeiss, Oberkochen.

## References

- [1] N. M. CEGLIO, A. M. HAWRYLUK, D. G. STEARNS, D. P. GAINES, R. S. ROSEN, and S. P. VERNON, *J. Vacuum Sci. Technol. B* **8**, 1325 (1990).
- [2] D. G. STEARNS, R. S. ROSEN, and S. P. VERNON, *J. Vacuum Sci. Technol. A* **9**, 2662 (1991).
- [3] H. NOMURA, K. MAYAMA, T. SASAKI, M. YAMAMOTO, and M. YANAGIHARA, *Proc. SPIE* **1720**, 395 (1992).
- [4] A. KLOIDT, K. NOLTING, U. KLEINEBERG, B. SCHMIEDESKAMP, U. HEINZMANN, P. MÜLLER, and M. KÜHNE, *Appl. Phys. Letters* **23**, 2601 (1991).
- [5] B. SCHMIEDESKAMP, A. KLOIDT, H. J. STOCK, U. KLEINEBERG, T. DÖHRING, M. PRÖPPER, S. RAHN, K. HILGERS, B. HEIDEMANN, T. TAPPE, U. HEINZMANN, M. KRUMREY, P. MÜLLER, F. SCHOLZE, and K. F. HEIDEMANN, *Opt. Engng.* **33**, 1314 (1994).
- [6] K. HOLLOWAY, K. B. DO, and R. SINCLAIR, *J. appl. Phys.* **65**, 474 (1989).
- [7] D. G. STEARNS, M. B. STEARNS, Y. CHENG, J. H. STITH, and N. M. CEGLIO, *J. appl. Phys.* **67**, 2415 (1990).
- [8] R. S. ROSEN, M. A. VILIARDOS, D. G. STEARNS, M. E. KASSNER, and S. P. VERNON, *Proc. SPIE* **1547**, 212 (1991).
- [9] H. J. STOCK, U. KLEINEBERG, B. HEIDEMANN, K. HILGERS, A. KLOIDT, B. SCHMIEDESKAMP, U. HEINZMANN, M. KRUMREY, P. MÜLLER, and F. SCHOLZE, *Appl. Phys. A* **58**, 371 (1994).
- [10] Z. JIANG, X. JIANG, W. LIU, and Z. WU, *J. appl. Phys.* **65**, 196 (1989).
- [11] A. I. FEDERENKO, S. D. FANCHENKO, V. V. KONDRATENKO, YU. P. PERSHIN, A. G. PONOMARENKO, E. N. ZUBAREV, and S. A. YULIN, *Handbook of Abstracts SRI 91*, Chester, 1991.
- [12] V. V. KONDRATENKO, YU. P. PERSHIN, O. V. POLTSEVA, A. I. FEDORENKO, E. N. ZUBAREV, S. A. YULIN, I. V. KOZHEVNIKOV, S. I. SAGITOV, V. A. CHIRKOV, V. E. LEVASHOV, and A. V. VINOGRADOV, *Appl. Optics* **32**, 1811 (1993).
- [13] H.-J. STOCK, U. KLEINEBERG, A. KLOIDT, B. SCHMIEDESKAMP, U. HEINZMANN, M. KRUMREY, P. MÜLLER, and F. SCHOLZE, *Appl. Phys. Letters* **63**, 2207 (1993).
- [14] A. K. PETFORD-LONG, M. B. STEARNS, C.-H. CHANG, S. R. NUTT, D. G. STEARNS, N. M. CEGLIO, and A. M. HAWRYLUK, *J. appl. Phys.* **61**, 1422 (1987).
- [15] B. L. HENKE, J. C. DAVIS, E. M. GULLIKSON, and R. C. PERERA, Lawrence Berkley Lab. LBL-26259, 1988.
- [16] B. HEIDEMANN, T. TAPPE, B. SCHMIEDESKAMP, and U. HEINZMANN, *Thin Solid Films* **228**, 60 (1993).

- [17] B. HEIDEMANN, T. TAPPE, B. SCHMIEDESKAMP, and U. HEINZMANN, *Appl. Surface Sci.* **78**, 133 (1994).
- [18] W. LOWELL MORGAN and D. B. BOERCKER, *Appl. Phys. Letters* **59**, 1176 (1991).
- [19] O. B. LOOPSTRA, E. R. VAN SNEK, TH. H. KEUSERS, and E. J. MITTERMEIJER, *Phys. Rev. B* **44**, 13519 (1991).
- [20] H. NAKAJIMA, H. FUJIMORI, and M. KOIWA, *J. appl. Phys.* **63**, 1046 (1988).
- [21] R. R. KOLA, D. L. WINDT, W. K. WASKIEWICZ, B. E. WEIR, R. HULL, G. K. CELLER, and C. A. VOLKERT, *Appl. Phys. Letters* **60**, 3120 (1992).
- [22] J. M. SLAUGHTER, P. A. KEARNEY, D. W. SCHULZE, C. M. FALCO, C. R. HILLS, E. B. SALOMAN, and R. N. WATTS, *Proc. SPIE* **1343**, 73 (1990).
- [23] M. B. STEARNS, C.-H. CHANG, and D. G. STEARNS, *J. appl. Phys.* **71**, 187 (1992).
- [24] A. GUIVARCH, P. AUVRAY, L. BERTHOU, M. LE CUN, J. P. BOULET, P. HENOC, G. PELOUS, and A. MARTINEZ, *J. appl. Phys.* **49**, 233 (1978).
- [25] S. OGURA, M. HAYASHIDA, A. ISHIZAKI, Y. KATO, and J. WOOD, *Proc. SPIE* **984**, 133 (1988).
- [26] Standard JCPDS diffraction pattern 17-917, ICDD, Swarthmore (PA) 1988.
- [27] J. Y. CHENG, H. C. CHENG, and L. J. CHEN, *J. appl. Phys.* **61**, 2218 (1987).

*(Received June 3, 1994)*